Deficiency in the Multicopy *Sycp3*-Like X-Linked Genes *Slx* and *Slxl1* Causes Major Defects in Spermatid Differentiation

Julie Cocquet,* Peter J. I. Ellis,† Yasuhiro Yamauchi,‡ Jonathan M. Riel,‡ Thomas P. S. Karacs,*§ Áine Rattigan,* Obah A. Ojarikre,* Nabeel A. Affara,† Monika A. Ward,‡ and Paul S. Burgoyne*

*Division of Stem Cell Biology and Developmental Genetics, Medical Research Council National Institute for Medical Research, Mill Hill, London NW7 1AA, UK; †Department of Pathology, Mammalian Molecular Genetics Group, University of Cambridge, Cambridge CB2 1QP, UK; and ‡Institute for Biogenesis Research, University of Hawaii Medical School, Honolulu, HI 96822

The human and mouse sex chromosomes are enriched in multicopy genes required for postmeiotic differentiation of round spermatids into sperm. The gene *Sly* is present in multiple copies on the mouse Y chromosome and encodes a protein that is required for the epigenetic regulation of postmeiotic sex chromosome expression. The X chromosome carries two multicopy genes related to *Sly*: *Slx* and *Slxl1*. Here we investigate the role of *Slx/Slxl1* using transgenically-delivered small interfering RNAs to disrupt their function. We show that *Slx* and *Slxl1* are important for normal sperm differentiation and male fertility. *Slx/Slxl1* deficiency leads to delay in spermatid elongation and sperm release. A high proportion of delayed spermatids are eliminated *via* apoptosis, with a consequent reduced sperm count. The remaining spermatozoa are abnormal with impaired motility and fertilizing abilities. Microarray analyses reveal that *Slx/Slxl1* deficiency affects the metabolic processes occurring in the spermatid cytoplasm but does not lead to a global perturbation of sex chromosome expression; this is in contrast with the effect of *Sly* deficiency which leads to an up-regulation of X and Y chromosome genes. This difference may be due to the fact that SLX/SLXL1 are cytoplasmic while SLY is found in the nucleus and cytoplasm of spermatids.

INTRODUCTION

Spermatogenesis is the process during which spermatogonial stem cells multiply and generate spermatocytes, which through two meiotic divisions form haploid spermatids that differentiate into spermatozoa. The differentiation of haploid round spermatids into spermatozoa (spermiogenesis) involves major alteration of cell structure and function as the nucleus is restructured *via* chromatin remodeling and compaction to form the sperm head, and sperm-specific structures, such as the acrosome and the flagellum, are formed (Russell *et al.*, 1990).

Abbreviation used: shRNAs, short hairpin RNAs.

The X and Y chromosomes are enriched in genes presumed to be important for sperm differentiation (Burgoyne and Mitchell, 2007; Mueller *et al.*, 2008) but functional studies remain rare (for review, see Stouffs *et al.*, 2009). The sex chromosomal complement of spermatid-expressed genes in man and mouse is enriched for multicopy genes (Skaletsky *et al.*, 2003; Toure *et al.*, 2005; Mueller *et al.*, 2008), and this has hindered gene function studies as a classical targeting strategy is not applicable (Burgoyne and Mitchell, 2007). Using an RNA interference–based strategy to disrupt the function of the multiple copies (>100) of the Y-encoded *Sly* (*Sycp3 like Y-linked*) gene, we found that its protein is crucial for the epigenetic regulation of sex chromosome expression after meiosis and for sperm differentiation (Cocquet *et al.*, 2009). The X chromosome carries two multicopy genes related to *Sly*: *Slx* (formerly known as *Xmr*; ~43 copies) and *Slx-like1* (*Slxl1*, formerly known as *AK015913* or *4930527E24Rik*; ~16 copies) (Reynard *et al.*, 2007; Scavetta and Tautz, 2010). Like *Sly*, *Slx* and *Slxl1* are specifically expressed in male postmeiotic germ cells. *Slx* encodes a cytoplasmic protein of unknown function, while for *Slxl1* it has been unclear whether transcripts are translated in the testis (Reynard *et al.*, 2007). In the case of *Sly* deficiency, *Slx* and *Slxl1* genes are up-regulated, along with other sex-chromosome genes, and thus are candidates to explain the aberrant sperm differentiation phenotypes and the near sterility of *Sly*-deficient males (Ellis *et al.*, 2005; Cocquet *et al.*, 2009). Intriguingly, genomic and genetic evidence suggests the existence of an

ongoing postmeiotic intragenomic conflict between multi-copy X and Y genes (Partridge and Hurst, 1998; Ellis and Affara, 2006), and *Slx* and *Sly* genes have been hypothesized to be key mediators of this 'competition' between X-bearing and Y-bearing gametes (Ellis *et al.*, 2005).

In the present study, we sought to determine the function of *Slx* and *Slxl1* and to see whether, like their Y-encoded counterpart *Sly*, they have a critical role in the control of sex chromosome expression during spermiogenesis. For this, we produced *Slx/Slxl1*-deficient mice using transgenically-delivered small interfering RNAs (siRNA). We show that the *Slx* gene family is important for normal mouse sperm differentiation (and thus for male fertility), but in contrast to *Sly* this is not a consequence of a global perturbation of sex chromosome expression.

MATERIALS AND METHODS

Plasmid Construction, Generation, and Breeding of Transgenic Mice

To generate the U6shSLX constructs, we used a PCR-based approach similar to that described in Harper *et al.*, 2005, using primers designed to generate the short hairpin SLX sequences (Harper *et al.*, 2005) (Supplementary Table 1). The PCR products were cloned into the pCR2.1 vector (TOPO TA Cloning, Invitrogen, Life technologies, Carlsbad, CA). An insulator element from the chicken β-globin domain (Chung *et al.*, 1993) and a genotype tag (gTag) were then added to each construct between SalI and BamHI restriction enzyme sites. These genotyping tags were inserted to enable discrimination of the different shSLX constructs by PCR (see Supplementary Table 1 for primer sequences). All constructs were sequenced before testing their specificity and efficiency.

Before injection, the plasmids were linearized at PvuI and BamHI sites and on-column purified from agarose gels (Gel Extract II kit, Macherey Nagel, Germany). Fertilized eggs from CBA/Ca × C57BL/10 matings were micro-injected with the construct, using standard protocols. Transgenic founders carrying an shSLX construct were identified by PCR and crossed with random-bred MF1 (National Institute for Medical Research colony) mice. Two founders (one male shSLX1 and one female shSLX2) transmitted the transgene to their offspring. The lines have been maintained by backcrossing shSLX transgenic females to MF1 XY^{RIII} males (i.e., with a Y chromosome originating from the RIII strain maintained on the random-bred MF1-NIMR background). Two-month-old MF1 XY^{RIII} males with (tsgic) and without (neg sib) the transgene were processed for all the analyses presented here except IVF, sperm motility, and electron microscopy for which males with a mixed B6D2F1 (C57BL/6 x DBA/2)/MF1 background were used. Animal procedures were in accordance with the United Kingdom Animal Scientific Procedures Act 1986 and were subject to local ethical review. For IVF, sperm motility, and electron microscopy, animal procedures were in accordance with the guidelines of the Laboratory Animal Services at the University of Hawaii and guidelines presented in the National Research Council's Guide for Care and Use of Laboratory Animals published by the Institute for Laboratory Animal Research of the National Academy of Science, Bethesda, MD, 1996.

Elutriation of Spermatids

Fractions enriched in round spermatids (>90%) were obtained using an adapted protocol of Meistrich (Meistrich, 1977), as described previously (Cocquet *et al.*, 2009).

Western Blot and Immunofluorescence

Western blot analyses were performed as described previously (Reynard *et al.*, 2007). Briefly, 10–15 micrograms of testis or spermatid fraction protein extracts were run on a 12% SDS/polyacrylamide gel or a 4–12% gradient Bis/Tris gel (NuPage, Invitrogen). After transfer and blocking, membranes were incubated overnight with either anti-SLX/SLXL1 antibody (Reynard *et al.*, 2007) diluted at 1/1000, anti–β-actin (SIGMA-Aldrich, St. Louis, MO) at 1/50000, or anti-GFP (Invitrogen) at 1/1000. Incubation with the corresponding secondary antibody coupled to peroxidase and detection by chemiluminescence were carried out as described by the manufacturer (SuperSignal West Pico, Pierce, Rockford, IL).

Immunofluorescence experiments were performed on testis material fixed in 4% buffered paraformaldehyde as described before (Cocquet *et al.*, 2009). Anti-SLX/SLXL1 antibody (Reynard *et al.*, 2007) and anti-H4K12ac (Millipore, Bedford, MA) were used overnight at 1/100. Testis sections were stained using an in situ cell death detection kit as described by the manufacturer (Roche Diagnostics, Indianapolis, IN). This detects apoptotic cells by fluorescently labeling DNA strand breaks (terminal deoxynucleotidyltransferase dUTP nick end labeling [TUNEL]). Approximately 100 tubules were counted per male (four individuals per genotype) to determine the percentage of tubules containing TUNEL-positive elongating/condensing spermatids. Alexa Fluor 594-conjugated peanut agglutinin lectin (Invitrogen), which stains the developing acrosome of spermatids, was used to stage the testis tubules.

Histology and Analysis of Sperm Head Morphology

For the analysis of spermatid development and sperm shedding delay, testes were fixed in Bouin (Sigma) and wax-embedded; five micron sections were stained with periodic acid–Schiff (PAS). Sperm smears obtained from the initial caput epididymis were silver stained and analyzed as described previously (Touré *et al.*, 2004). Sperm count was done on cauda epididymis. Sperm count, assessment of sperm morphology, and timing of sperm shedding were performed on two-month-old animals (at least four mice per genotype). Transmission electron microscopy was done on sperm from the cauda epididymis as previously described (Yamauchi *et al.*, 2010).

Fertility Testing and In Vitro Fertilization

To assess fertility, six MF1 XY^{RIII} males of each genotype were mated with MF1 females over a period of six and a half months. Mating was confirmed by the presence of copulatory plugs. In vitro fertilization (IVF) analysis was performed with sperm from four shSLX1 males, six shSLX2 males, and six nontransgenic siblings (WT) from a mixed B6D2F1/MF1 background, using B6D2F1 oocytes as described before (Cocquet *et al.*, 2009). Sperm from the same males were subjected to motility analysis.

Real-Time PCR and Microarray Analyses

For real-time Reverse Transcription-Polymerase Chain Reaction (RT-PCR) and microarray analyses, RNA was extracted from total testis or from fractions of 1×10^6 round spermatids using Trizol (Invitrogen). Reverse transcription of polyadenylated RNA and real-time PCR were performed as described previously (Cocquet *et al.*, 2009). Briefly, real-time PCR was performed using Absolute qPCR SYBR Green ROX mix (ThermoFisher Scientific, Waltham, MA) on an ABI PRISM 7500 machine (Applied Biosystems, Life technologies, Carlsbad, CA). Testis samples from four to five transgenic mice and six nontransgenic siblings (negative controls), all at two months of age, were analyzed. All reactions were carried out in triplicate per assay and *Acrv1* (an autosomal spermatid specific gene) was included on every plate as a loading control. The difference in PCR cycles with respect to *Acrv1* (ΔCt) for a given experimental sample was subtracted from the mean ΔCt of the reference samples (negative siblings) ($\Delta\Delta$Ct). For quantification on purified round spermatid samples, β-*actin* was used as the loading control. Primer sequences are available in Supplementary Table 1.

Microarray analyses were performed on RNA from purified round spermatid fractions as previously described (Cocquet *et al.*, 2009) using two groups (a pool of 2–4 individuals) of shSLX1 transgenic mice and four groups of WT mice. Results were compared with those obtained with purified round spermatid fractions from *Sly*-deficient males (Cocquet *et al.*, 2009). Differentially expressed genes were classified according to their likely biological function in Onto-Express.

Statistical Analysis

For comparisons of the incidence of sperm head abnormalities, differences between genotypes were assessed by ANOVA after angular transformation of percentages, using the Generalized Linear Model provided by NCSS statistical data analysis software. The same test was applied to the frequency of abnormal head-tail connections, the proportion of oocytes fertilized in vitro, tubules with sperm shedding delay, TUNEL+ elongating spermatids, abnormal H4K12Ac staining, or sperm motility. Student's *t* test was used to compare the data obtained for fecundity, sperm number, testis weight, Western blot quantification, and real-time PCR (performed on the $\Delta\Delta$Ct values). For microarray analysis, quantile normalization of all expression data was performed using BeadStudio (Illumina Inc., San Diego, CA). Data for the shSLX1/control spermatids was compared in BeadStudio, using the Illumina custom error model. Significant up- or down-regulation was defined as a false discovery rate-corrected *p* value of ≤0.05 and a fold change of ≥1.5.

RESULTS

Specific Knockdown of Slx and Slxl1 Transcripts by Transgenically-Delivered siRNAs

To study the function of the *Slx* multicopy gene family, we used a strategy similar to the one previously developed for *Sly* (Cocquet *et al.*, 2009), i.e., the transgenic delivery of short hairpin RNAs (shRNAs) that generate small interfering RNAs (siRNAs). These siRNAs mediate gene-specific knockdown *via* RNA interference. In our strategy, the shRNAs are
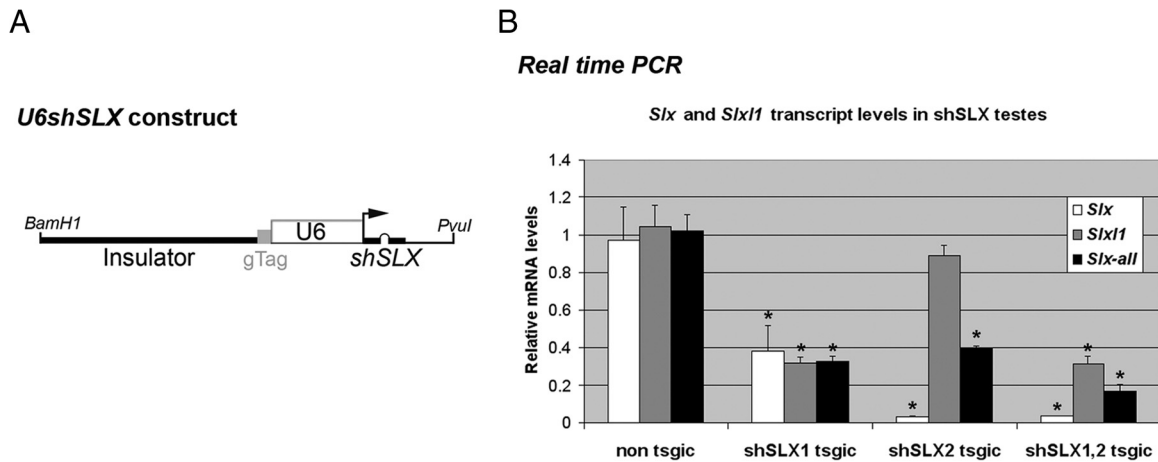
A

U6shSLX construct

B

Real time PCR

Slx and Slxl1 transcript levels in shSLX testes

Figure 1. Transgenically delivered shSLX constructs knockdown *Slx* and *Slx-like1* at the transcript level. (A) Structure of the shSLX construct. The U6 promoter drives the expression of a short hairpin RNA targeting *Slx/Slxl1* (shSLX). An insulator sequence is located upstream of the U6 promoter. A 'genotyping' tag (gTag) that is specific to each shSLX construct has been inserted to facilitate genotyping in double transgenic mice. (B) Quantification of the knockdown of *Slx* and *Slxl1* transcripts in shSLX testes by real-time RT-PCR. Values were normalized to *Acrv1* (an autosomal spermatid-specific gene). '*Slx-all*' represents amplification with primers designed to amplify both *Slx* and *Slxl1* transcripts. One star indicates significant difference from nontransgenic (WT) value ($p < 0.005$; t test).

expressed under the control of the strong and ubiquitous U6 promoter (Figure 1).

Four shRNA sequences expected to target *Slx* and *Slx-like 1* (*Slxl1*) transcripts were carefully selected (to avoid cross-reaction with related sequences such as *Sly* and *Xlr*) and used to design shRNA constructs. The efficiency and specificity of these shRNA constructs were tested in cell culture by cotransfection (Supplementary Figure 1). Based on these results, two efficient and specific shRNA constructs (shSLX1 and shSLX2) were used to produce transgenic mice *via* pronuclear injection. Each transgene was stably inserted in the genome and was transmitted to the progeny. The resulting transgenic lines (designated shSLX1 and shSLX2) showed a dramatic knockdown of *Slx* transcripts: ~62% decrease in shSLX1 testes and ~97% decrease in shSLX2 testes, as quantified by real-time PCR (Figure 1). The shSLX2 transgene did not have a significant effect on *Slxl1* expression; however, shSLX1 testes displayed a ~68% decrease in *Slxl1* transcript level. These results are in agreement with predictions from cotransfection experiments (cf. Supplementary Figure 1). Males carrying both shSLX1 and shSLX2 transgenes (shSLX1,2 transgenic mice) had decreased levels in both *Slx* and *Slxl1* transcripts (~97% and ~69% decrease, respectively). When using primers designed to amplify together *Slx* and *Slxl1* transcripts (*Slx-all*), global knockdown was estimated as ~68% for shSLX1, ~59% for shSLX2, and ~83% for shSLX1,2.

SLX and SLXL1 Protein Levels Are Reduced in shSLX Testes

Two antibodies had been developed for the study of SLX (Reynard *et al.*, 2007). In cell lines transiently expressing an *Slx* or *Slxl1* transgene, one antibody (anti-SLX aka anti-SLX[69-81]) detected specifically SLX protein, while the other (anti-SLX/SLXL1 aka anti-SLX[96-106]) detected both SLX and SLXL1 protein. In testes, SLX protein was detected by both antibodies but it remained unclear whether *Slxl1* transcripts were translated (Reynard *et al.*, 2007). Making use of our two shSLX mouse lines (shSLX1 targeting *Slx* and *Slxl1* transcripts, and shSLX2 only targeting *Slx*) we decided to rein-

vestigate *Slxl1* translation. SLX protein is predicted to be 25 kDa, while SLXL1 is expected at 18 kDa. After separation on a 12% polyacrylamide gel, Western blot detection with anti-SLX specific antibody showed a fainter band in shSLX1 testis protein samples compared with wild-type testes (i.e., nontransgenic siblings). In shSLX2 testes, the band was barely visible (Figure 2A) in agreement with transcript quantifications. Detection with the anti-SLX/SLXL1 antibody showed a double band of reduced intensity in shSLX1 and shSLX2 testes (Figure 2A). After separation on a 4–12% gradient gel, it became clear that the upper band (indicated by the gray arrowhead) corresponds to SLX protein (decreased in shSLX1 and in shSLX2 testes) while the bottom band (indicated by the black arrowhead) corresponds to SLXL1 protein (reduced in shSLX1 but almost unaffected in shSLX2 testes). As expected, double transgenic shSLX1,2 mice showed a deficiency in both types of proteins. Similar results were obtained on round spermatid protein extracts (Figure 2B). Immunofluorescence on testis section using anti-SLX/SLXL1 antibody confirmed a dramatic decrease in SLX/SLXL1 protein levels in round spermatids (Supplementary Figure 2).

All in all, we have produced mouse models deficient for *Slx/Slxl1* genes. We proceeded to analyze their phenotypes to elucidate the roles of these genes in spermiogenesis and the extent to which *Slx/Slxl1* depletion mimics *Sly* deficiency.

Slx/Slxl1 Deficiency Leads to Impaired Male Fertility

The first phenotype of *Slx/Slxl1*-deficient males we observed was poor fertility. Over a breeding period of 6½ months with young WT (MF1) females, shSLX1 and shSLX2 males had a considerable reduction in the number of litters and in litter sizes compared with WT males (nontransgenic siblings) (Table 1). Double transgenic shSLX1,2 males were sterile. Transgenic females did not have obvious breeding problems (data not shown). In vitro, the fertilizing ability of *Slx/Slxl1*-deficient epididymal sperm was also severely impaired relative to controls (Table 1). Testis weight for shSLX1 and shSLX2 males did not differ from controls but shSLX double transgenic testes were slightly smaller (90 mg vs. 102 mg in WT) (Table 1).
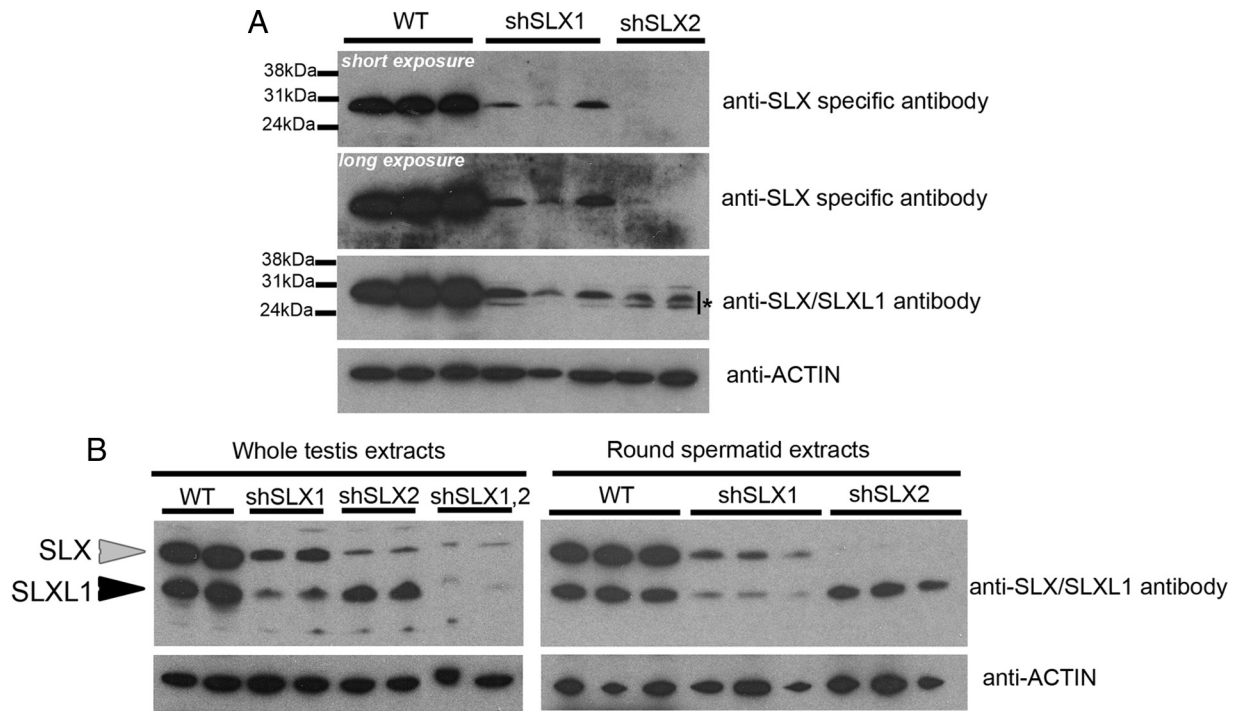
Figure 2. Transgenically delivered shSLX constructs lead to a dramatic decrease of SLX and SLXL1 proteins. (A) Western blot detection of SLX/SLXL1 proteins on WT (i.e., nontransgenic siblings), shSLX1 and shSLX2 adult testicular extracts, after separation by 12% PAGE. A double band (indicated by a star) can be observed when detecting with the anti-SLX/SLXL1 antibody. Actin antibody was used for normalization. (B) Left panel, Western-blot detection of SLX/SLXL1 proteins on WT, shSLX1, shSLX2, and shSLX1,2 adult testicular extracts, after separation by 4–12% gradient PAGE. The upper band (gray arrowhead) corresponds to SLX protein. The bottom band (black arrowhead) is SLXL1 protein. Similar results were obtained on purified round spermatid extracts from WT, shSLX1, and shSLX2 mice (right panel, same conditions). Actin antibody was used for normalization.

Slx/Slxl1 Deficiency Leads to Abnormal Spermatid Elongation

We sought to determine the origin of the fertility defect observed in shSLX males. Histology of all types of *Slx/Slxl1*-deficient males did not differ from WT until post-meiotic stages. This is in agreement with the observation that *Slx* and *Slxl1* expression is restricted to the postmeiotic stage of male germ cells (i.e., spermatids) (Reynard *et al.*, 2007). There was no detectable delay of round spermatid development; however, *Slx/Slxl1*-deficient testes had a defect in spermatid elongation (from stage IX and onwards). For instance, in PAS-stained stage XII tubules of *Slx/Slxl1*-deficient mice, elongating spermatids are visibly less developed (with the presence of step10 spermatids instead of step12) than in controls (Figure 3, A and C). Histone H4 hyperacetylation is a good marker of the spermatid elongation stages, as it occurs in early elongating spermatids before histone replacement by transition proteins (Hazzouri *et al.*, 2000; Gaucher *et al.*, 2009). Using antibodies directed against acetylated lysine 8 and 12 of histone H4 (H4K8Ac and H4K12Ac) as markers

Table 1. Analysis of the reproductive parameters of *Slx/Slxl1*-deficient males and controls

Parameters	Characteristics from males with following genotypes			
	WT	shSLX1	shSLX2	shSLX1,2
Number of litters per male[a]	6	1.83*	3.33*	0*
Total number of offspring per male[a]	70.17	9.83*	18.83*	0*
Average litter size[a]	11.8	3.92*	4.26*	0*
Oocytes fertilized in vitro (%)	54.5	4.6**	1.0**	N/D
Testis weight (mean value in mg ± SEs)	102.3 ± 2.5	99.8 ± 3.0	104.1 ± 3.1	90.1* ± 3.4
Total motile sperm (%)	46.3	25.4**	22.9**	N/D
Sperm number/cauda (mean value × 10^{-6} ± SEs)				
MF1	13.6 ± 0.8	2.0* ± 0.8	6.6* ± 1.2	0.2* ± 0.1
B6D2F1	7.0 ± 1.8	5.9 ± 1.9	5.2 ± 2.0	N/D

[a] Six males of each genotype were mated with MF1 females over a period of six and a half months.

* Significantly different from WT ($p < 0.05$; *t* test).

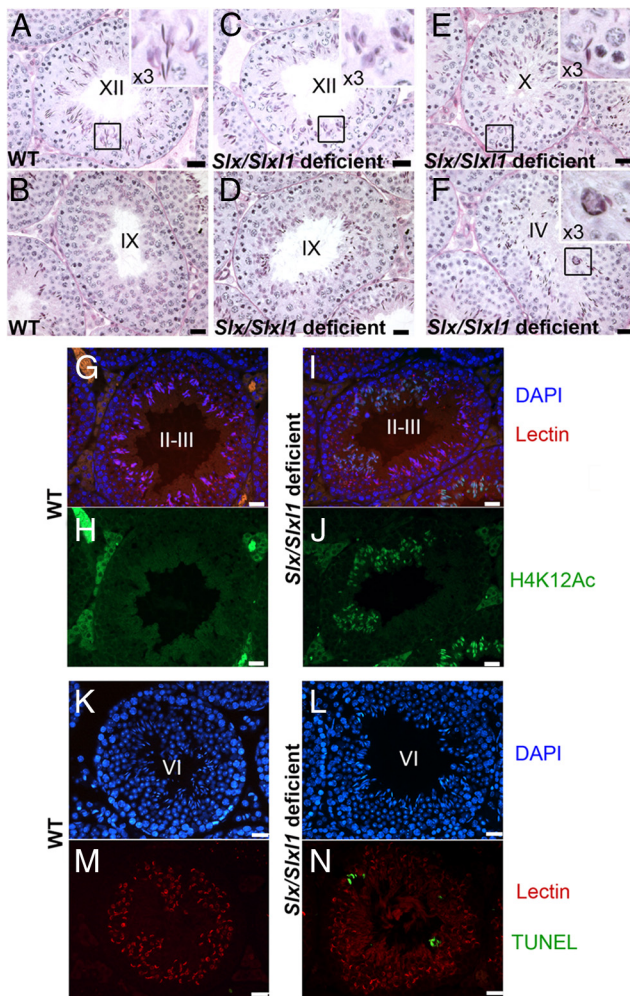** Significantly different from WT ($p < 0.05$; ANOVA).

Figure 3. Impaired spermiogenesis and increased apoptosis of elongating spermatids in *Slx/Slxl1*-deficient mice. (A–D) In PAS-stained stage XII testis tubules of *Slx/Slxl1*-deficient (shSLX1 transgenic) mice, elongating spermatids are less developed than in controls (A). Typically, elongating spermatids with morphology of step 10 spermatids were observed in step XII tubules (C). In PAS-stained stage IX testis tubules of *Slx/Slxl1*-deficient mice (D) mature sperm are retained in stage IX tubules, whereas in WT testes (B) mature sperm have already been released into the lumen. (E) PAS-stained stage X *Slx/Slxl1*-deficient testis tubule. Several mature sperm are retained near the basal lamina (enlargement, right top corner). (F) PAS-stained stage IV *Slx/Slxl1*-deficient testis tubule. A typical group of dying sperm organized in circle can be observed (enlargement, right top corner). (G–J) stage II-III testis tubules of *Slx/Slxl1*-deficient mice present a great number of delayed elongating spermatids (marked with H4K12Ac antibody in green). Same stage tubules of control mice do not show any remaining H4K12Ac signal in spermatids. (K–M) Detection of apoptosis (TUNEL) in WT and *Slx/Slxl1*-deficient testes. Representative pictures show the presence of several apoptotic elongating spermatids (in green) in a stage VI testis tubule of a *Slx/Slxl1*-deficient male. No or very few apoptotic cells can be observed in a control testis (shSLX nontransgenic sibling). DAPI (in blue) was used to stain nuclei, and Lectin (in red) was used to stage the seminiferous tubules. Scale bar, 20 μm.

of stage 9–12 elongating spermatids, we observed a major delay in spermatid elongation (Figure 3, G–J): H4K12Ac positive spermatids were retained in ~70% of stage I to IV tubules in shSLX1 testes, 11% in shSLX2 and 93% in shSLX1,2, versus 4% in WT (shSLX1 and shSLX1,2 values significantly different from WT; ANOVA, $p < 0.0001$).

Slx/Slxl1 Deficiency Leads to Delay in Sperm Shedding and Reduction of Sperm Count

We then observed that mature (step 16) sperm were retained in most stage IX to XI tubules, instead of being normally shed at stage VIII (Figure 3, B and D). The occurrence of sperm shedding delay was significantly higher in *Slx/Slxl1*-deficient males compared with WT (95 and 77% of stage IX to XI tubules with retained sperm in shSLX1 and shSLX2 males respectively vs. 12% in WT; ANOVA $p < 0.0005$). Interestingly, a delay in sperm shedding has previously been observed in *Sly*-deficient mice and MSYq-deficient mice (Touré *et al.*, 2004; Cocquet *et al.*, 2009), but in these cases the unshed sperm were located adjacent to, and were eventually released into, the lumen; in *Slx/Slxl1*-deficient tubules, unshed sperm were often located near the basal lamina or form a group of dying cells (Figure 3, E and F). Apoptotic (TUNEL-positive) elongating spermatids were found in all types of tubule stages of the seminiferous epithelium cycle (Figure 3, K–N, and Supplementary Figure 4). The proportion of testicular tubules containing TUNEL-positive elongating/condensing spermatids was determined and found to be significantly higher in *Slx/Slxl1*-deficient testes compared with controls (~70% in shSLX1 and shSLX1,2 testes, ~25% in shSLX2 testes vs. ~3% in WT; ANOVA, $p < 0.0005$). The substantial loss of these spermatids was associated with reduced sperm counts in cauda epididymis from *Slx/Slxl1*-deficient males (Table 1).

Slx/Slxl1-Deficient Sperm Are Abnormally Formed and Exhibit Reduced Motility

Analysis of *Slx/Slxl1*-deficient epididymis revealed a significant increase in the incidence of abnormal sperm with ~49% of spermhead abnormalities in shSLX1 and ~36% in shSLX2 (vs. ~8% in WT; ANOVA, $p < 0.0005$) (Figure 4, A and B; Supplementary Figure 3). In addition to spermhead malformations, shSLX1 and shSLX2 spermatozoa displayed abnormal head to tail connections (values significantly different from WT; ANOVA, $p < 0.005$) (Figure 4, C and D). Using electron microscopy, we observed epididymal sperm with partially detached heads or abnormally-oriented tails: either aligned parallel to the head, curved or looped (Figure 4, E–J). Abnormal connection between the spermhead and its tail could have an effect on sperm motility, and, indeed, sperm motility was impaired as shown by the decrease in the proportion of motile sperm (Table 1).

Transcriptome Analyses Show that Slx/Slxl1 Deficiency Alters Metabolic Processes Occurring in the Spermatids

To better understand the consequences of *Slx/Slxl1* deficiency, we performed microarray analyses on purified round spermatids (the site of *Slx* and *Slxl1* expression) from shSLX1 mice and controls. First, this analysis confirmed the knockdown of *Slx* and *Slxl1* transcripts. Second, in *Slx/Slxl1*-deficient round spermatids, 101 genes were found to be significantly up-regulated compared with controls. Of these 101 genes, 77 are annotated and, of these, 54% (42/77) encode proteins involved in various metabolic processes, among which are the serine proteases belonging to *Kallikrein 1* family (*klk1*, *klk1b26*, *klk1b5*, *klk1b9*, *klk1b4*, *klk1b27*) and *Ela2a*; several enzymes implicated in lipid metabolism (*Acsl5*, *Cyp2a12*, *St8sia5*, *Agpat2*, *Ppap2b*) and energy metabolism (*Nqo2*, *Atp6v1h*, *4933437F05Rik*); and proteins of the ubiquitin pathway (*Usp3*, *Ube2g2*). Several genes coding for proteins of the cytoskeleton and the extracellular matrix (classified in category 'cellular component organization') were also affected by *Slx/Slxl1* deficiency such as *Tmod4*
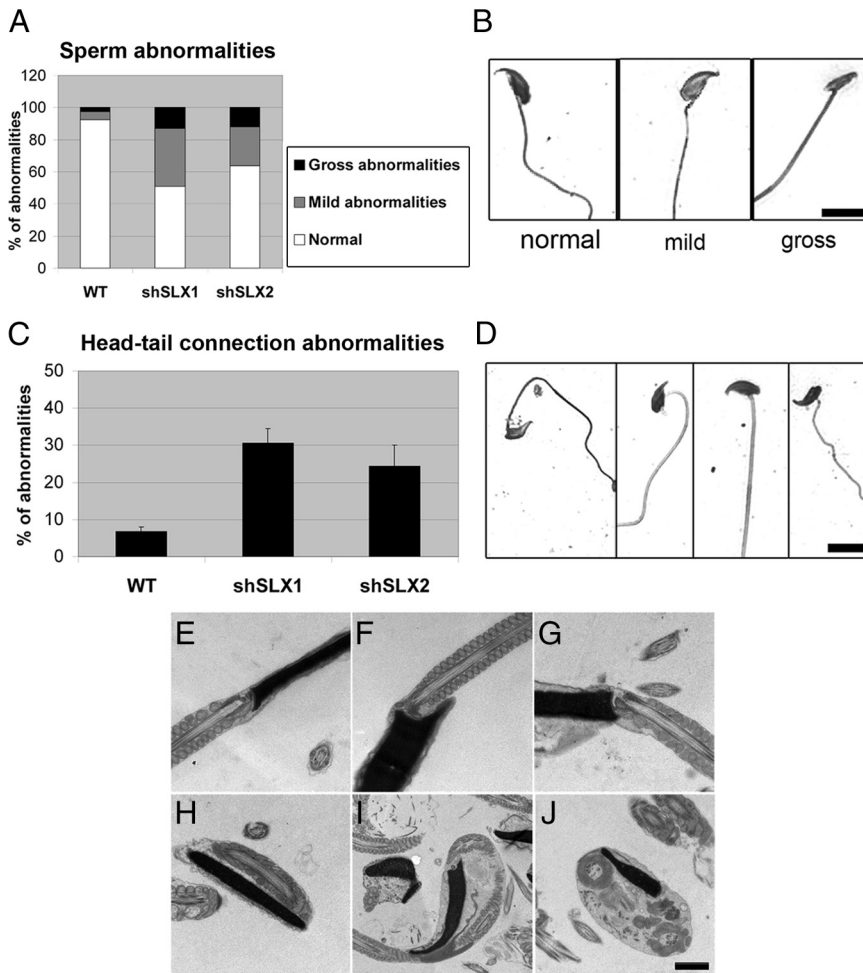
Figure 4. Sperm abnormalities in *Slx/Slxl1*-deficient mice. (A) Bar graph representing the percentage of sperm with sperm head abnormalities in *Slx/Slxl1*-deficient mice and control. (B) Examples of sperm head abnormalities observed in *Slx/Slxl1*-deficient mice (silver-stained epididymal sperm). Scale bar, 10 μm. (C) Bar graph representing the percentage of sperm with abnormal head-tail connections in epididymal sperm from *Slx/Slxl1*-deficient mice and control. (D) Examples of head-tail connection anomalies in *Slx/Slxl1*-deficient spermatozoa. Scale bar, 10 μm. (E–J) Electron microscopy pictures of WT (E and F) and *Slx/Slxl1*-deficient epididymal sperm with partial detachment of the tail (G), parallel alignment of the head and tail (H), curved tail (I), or looped tail (J). Pictures were taken using the same parameters. Scale bar, 1 μm.

(*Tropomodulin 4*), *Myl2* (*myosin light chain 2*), *Col20a1* (*collagen, type XX, alpha 1*), *Pstpip1* (*proline-serine-threonine phosphatase interacting protein 1*), which is a member of the actin-associated protein family (Spencer *et al.*, 1997), and *LOC100045019* (similar to *Tubulin, gamma 2*) (Figure 5A). Interestingly, several genes involved in positive or negative regulation of apoptosis were also found affected (such as *Hipk2*, *Tnfsf13b*, *Jund1*). Complete results can be found in Supplementary Figure 5.

Slx/Slxl1 Deficiency Does Not Lead to Global Perturbation of Sex Chromosome Gene Expression

Slx and *Slxl1* genes are related to the Y-encoded *Sly* multicopy gene. SLY protein has been shown to repress sex chromosome genes in spermatids and, as a result, X- and Y-encoded transcripts are up-regulated in the case of *Sly* deficiency (Cocquet *et al.*, 2009). Here, in round spermatids from *Slx/Slxl1*-deficient males, none of the genes found up-regulated were located on the sex chromosomes (Figure 5B). Only one X-encoded transcript (apart from *Slx* and *Slxl1* transcripts and cross-hybridization with an 'Sly' probe), *Wdr13*, was found significantly down-regulated in *Slx/Slxl1*-deficient round spermatids. Real-time PCR analysis on *Slx/Slxl1*- and *Sly*-deficient round spermatid fractions confirmed that *Wdr13* is differentially regulated by SLY and SLX/SLXL1 (Figure 5C).

DISCUSSION

Using an siRNA approach to produce mice with markedly reduced transcript levels for the multicopy genes *Slx* and *Slxl1*, we have demonstrated that the *Slx* gene family is important for normal mouse sperm development. *Slx/Slxl1* deficiency considerably delays spermatid elongation and sperm release in the lumen. These perturbations of sperm differentiation are associated with the elimination of many elongating/condensing spermatids *via* apoptosis, with a consequent reduced sperm count. The remaining spermatozoa are abnormally shaped and have decreased motility and fertilizing abilities. All these factors are likely to contribute together to the near sterility observed in *Slx/Slxl1*-deficient males.

Microarray analyses revealed that *Slx/Slxl1* deficiency does not lead to global up-regulation of X- and Y-linked genes after meiosis; this is in striking contrast with what we had observed in the case of *Sly* deficiency, where the vast majority of the genes found up-regulated were encoded either by the X or Y chromosome (Cocquet *et al.*, 2009). This difference may stem from the fact that i) SLX/SLXL1 proteins are restricted to the cytoplasm while SLY is found in both the nucleus and cytoplasm of spermatids (Reynard *et al.*, 2007; Cocquet *et al.*, 2009); ii) SLX/SLXL1 only share ~43% overall homology with SLY (while SLX and SLXL1 share ~66% identity).
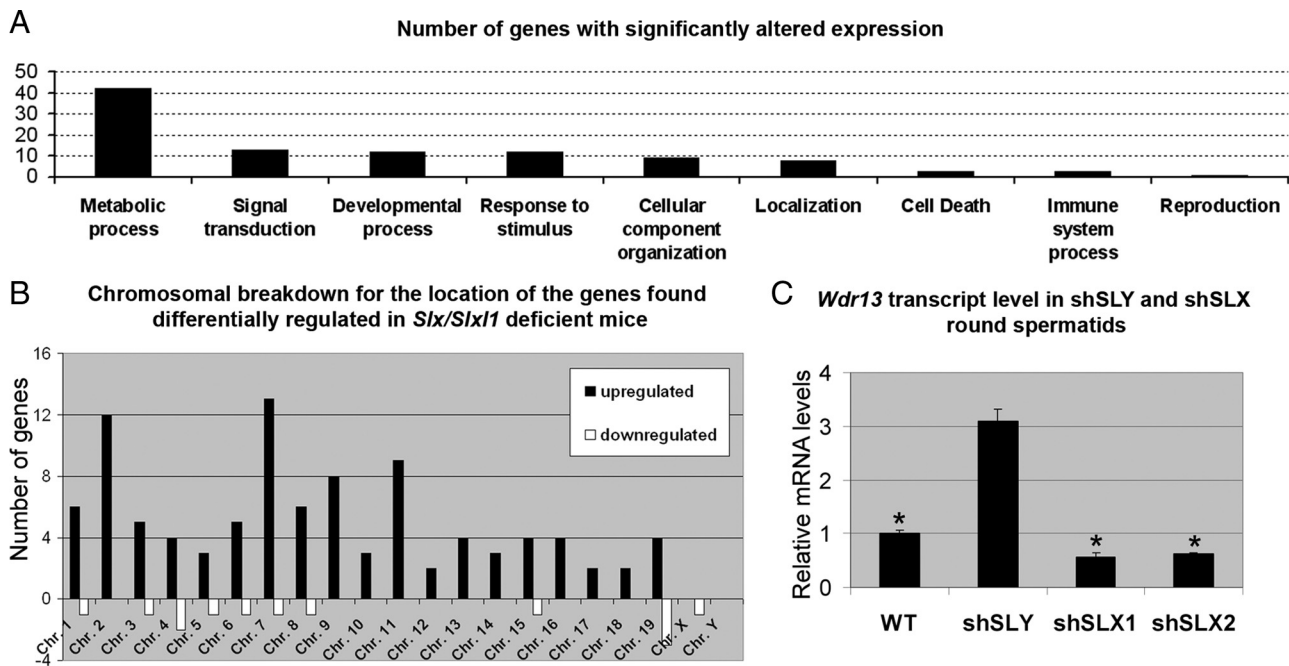
A

Number of genes with significantly altered expression

B

Chromosomal breakdown for the location of the genes found differentially regulated in *Slx/Slxl1* deficient mice

C

***Wdr13* transcript level in shSLY and shSLX round spermatids**

Figure 5. Transcriptome analysis of *Slx/Slxl1*-deficient round spermatids versus WT round spermatids. (A) Bar graph representing the number of genes found differentially expressed in round spermatids from *Slx/Slxl1*-deficient males compared with those of WT males by microarray. Differentially expressed genes are shown by classification according to their likely biological function in Onto-Express. (B) Chromosome location of the genes found up- or down-regulated in case of *Slx/Slxl1* deficiency. Note the enrichment of up-regulated genes on chromosome 7. This is due to the presence of the *Klk1* genes that are affected by the loss of *Slx/Slxl1*. (C) Quantification of the transcript level of the X-encoded *Wdr13* gene in purified round spermatids of shSLY, SLX1, shSLX2, and WT males by real-time RT-PCR. Values were normalized to β-actin. One star indicates significant difference from WT value ($p < 0.05$; t test). *Wdr13* transcript level is differentially affected by *Slx/Slxl1* or *Sly* deficiency.

Only a few genes (mainly *kallikrein 1-related* genes) were found up-regulated in both models (*Slx/Slxl1*- and *Sly*-deficient males). Kallikrein-related peptidases are serine proteases with a variety of physiological roles; they have notably been reported to be involved in semen liquefaction and consequently in sperm motility but through their production by the prostate (Emami *et al.*, 2009). Their biological role in the testis remains to be defined, but they could act (as they do in other contexts) as signaling molecules (for review, see Sotiropoulou *et al.*, 2009). Interestingly, *kallikrein 1–related* transcripts are also found up-regulated in mouse models with deletions of the Y long arm (which represents a non siRNA model of *Sly* deficiency) (Cocquet *et al.*, 2009).

Among the few genes that were found differentially affected by *Slx/Slxl1* and *Sly* deficiency (i.e., up-regulated in one model and down-regulated in the other) are *Fndc3* and *Wdr13*. *Fndc3* has been implicated in spermatid–Sertoli cell adhesion (Obholz *et al.*, 2006). *Wdr13* is predominantly expressed in male germ cells, but its function is yet unknown (Singh *et al.*, 2003; Suresh *et al.*, 2005). Future work (such as gain or loss of function approaches) will be required to determine the contribution of these candidate genes to the spermiogenic phenotype(s) observed in *Slx/Slxl1*- and *Sly*-deficient males.

In the case of *Sly* deficiency, ~100 X and Y-linked spermiogenic genes are up-regulated, among which are *Slx* and *Slxl1* (Cocquet *et al.*, 2009). Both *Slx/Slxl1*-deficient males and *Sly*-deficient males present sperm differentiation defects, though some of these defects appear to be specific to *Slx/Slxl1* deficient males, such as spermatid elongation delay and abnormal head-tail connections. The increase of *Slx* and *Slxl1* transcript levels are likely to contribute to the spermio-

genic defects observed in *Sly*-deficient males. *Slx* and *Sly* genes have been hypothesized to be involved in an intragenomic conflict occurring between X-bearing and Y-bearing gametes (Ellis *et al.*, 2005). The production of double transgenic mice deficient for both *Slx/Slxl1* and *Sly* would address this question.

The structural changes, such as acrosome and flagellum formation, that lead to the transformation of a round cell into a highly specialized sperm cell start soon after meiosis in the round spermatid (Russell *et al.*, 1990). Many of the genes found altered in our microarray analysis of *Slx/Slxl1*-deficient round spermatids encode enzymes associated with specific cellular organelles and involved in various metabolic processes (such as energy production, ubiquitin-mediated degradation, etc.). Several proteins of the cytoskeleton were also affected. These results suggest that a 'cytoplasmic' defect underlies the above-mentioned sperm differentiation abnormalities. The mechanism by which SLX/SLXL1 proteins regulate these processes remains mysterious as no functional domain (apart from the Cor1 domain) is known and previous attempts to identify potential protein partners have failed (L Reynard and P Burgoyne, unpublished data). Because SLX/SLXL1 proteins are restricted to the spermatid cytoplasm, it is unlikely that the genes found altered in our microarray analysis are direct transcriptional targets of SLX/SLXL1. One attractive hypothesis is that a yet unidentified partner of SLX/SLXL1 is at the basis of the transcriptional changes that are necessary for normal spermatid elongation.

Finally, before the elimination of elongating spermatids by apoptosis, several 'cell death' genes were found altered in round spermatids deficient for *Slx/Slxl1*. *Hipk2*, a potentiator of p53-mediated transcriptional activation of proapoptotic

genes (Hofmann *et al.*, 2002), was up-regulated while the proto-oncogene *Jund1* was down-regulated. SLX/SLXL1 may consequently be important for the balance between cell proliferation/differentiation and cell death during sperm development. This relates to a recent study in which expression in tumor cells of SYCP3, SLX, or the related protein XLR was shown to induce activation of AKT and up-regulation of antiapoptotic proteins (Kang *et al.*, 2010). Ectopic expression of SYCP3 was found in some human cancers (such as cervical cancer and acute leukemia) (Niemeyer *et al.*, 2003; Kang *et al.*, 2010). AKT proteins are known to have a crucial role in cell proliferation, survival, and differentiation in many tissues (Manning and Cantley, 2007). In the testis, the phosphatidylinositol 3-kinase (Pi3k)/AKT pathway has been shown to be required for spermatogonial stem cell survival and proliferation (Blume-Jensen *et al.*, 2000; Chen *et al.*, 2001). To our knowledge, the impact of the Pi3k/AKT pathway on spermatid development and differentiation remains unclear, but AKT1 protein has been described to be present and activated (phosphorylated) at different stages of the rat germ cell development, including spermatids (Hixon and Boekelheide, 2003). Interestingly, several genes involved in the AKT regulation cascade were found up-regulated in round spermatids deficient for *Slx/Slxl1*: *Eif4ebp1* is a gene of the Pi3K signaling pathway and acts downstream of AKT/PKB; while *Tnfsf13b* (aka *Baff*) and *Aatf* encode two positive regulators of AKT (Otipoby *et al.*, 2008; Ishigaki *et al.*, 2010). The mechanism by which SLX/SLXL1 acts upon the Pi3k/AKT pathway in postmeiotic germ cells or in case of ectopic activation remains to be determined.

In conclusion, our work provides insight into the function of multicopy X-linked genes. With the transgenic-delivery of siRNA we have targeted both *Slx* and *Slxl1* transcripts and characterized their biological role in spermatogenesis. To the best of our knowledge, our study is the first to describe the targeted disruption of the function of X chromosome-encoded multicopy genes in mammals. A similar strategy could be applied to the study of other multicopy genes such as the numerous 'cancer/testis antigens' found on the X chromosome for which a role in germ cells remains largely unknown (for review, see Simpson *et al.*).

ACKNOWLEDGMENTS

REFERENCES

Blume-Jensen, P., Jiang, G., Hyman, R., Lee, K. F., O'Gorman, S., and Hunter, T. (2000). Kit/stem cell factor receptor-induced activation of phosphatidylinositol 3'-kinase is essential for male fertility. Nature Genet. *24*, 157–162.

Burgoyne, P. S., and Mitchell, M. J. (2007). The roles of mouse Y chromosome genes in spermatogenesis. In: Y Chromosome and Male Germ Cell Biology, eds. Y.-F.C. Lau and W.Y. Chan, Hackensack, NJ: World Scientific Publishers, 27–45.

Chen, W. S., Xu, P. Z., Gottlob, K., Chen, M. L., Sokol, K., Shiyanova, T., Roninson, I., Weng, W., Suzuki, R., Tobe, K., Kadowaki, T., and Hay, N. (2001). Growth retardation and increased apoptosis in mice with homozygous disruption of the Akt1 gene. Genes Dev. *15*, 2203–2208.

Chung, J. H., Whiteley, M., and Felsenfeld, G. (1993). A 5' element of the chicken beta-globin domain serves as an insulator in human erythroid cells and protects against position effect in Drosophila. Cell *74*, 505–514.

Cocquet, J., Ellis, P. J., Yamauchi, Y., Mahadevaiah, S. K., Affara, N. A., Ward, M. A., and Burgoyne, P. S. (2009). The multicopy gene Sly represses the sex chromosomes in the male mouse germline after meiosis. PLoS Biol. *7*, e1000244.

Ellis, P. J., and Affara, N. A. (2006). Spermatogenesis and sex chromosome gene content: an evolutionary perspective. Hum. Fertil. (Camb) *9*, 1–7.

Ellis, P.J.I., Clemente, E. J., Ball, P., Toure, A., Ferguson, L., Turner, J.M.A., Loveland, K. L., Affara, N. A., and Burgoyne, P. S. (2005). Deletions on mouse Yq lead to upregulation of multiple X- and Y-linked transcripts in spermatids. Hum. Mol. Genet. *14*, 2705–2715.

Emami, N., Scorilas, A., Soosaipillai, A., Earle, T., Mullen, B., and Diamandis, E. P. (2009). Association between kallikrein-related peptidases (KLKs) and macroscopic indicators of semen analysis: their relation to sperm motility. Biol. Chem. *390*, 921–929.

Gaucher, J., Reynoird, N., Montellier, E., Boussouar, F., Rousseaux, S., and Khochbin, S. (2009). From meiosis to postmeiotic events: The secrets of histone disappearance. FEBS J. *277*, 599–604.

Harper, S. Q., Staber, P. D., He, X., Eliason, S. L., Martins, I. H., Mao, Q., Yang, L., Kotin, R. M., Paulson, H. L., and Davidson, B. L. (2005). RNA interference improves motor and neuropathological abnormalities in a Huntington's disease mouse model. Proc. Natl. Acad. Sci. USA *102*, 5820–5825.

Hazzouri, M., Pivot-Pajot, C., Faure, A. K., Usson, Y., Pelletier, R., Sele, B., Khochbin, S., and Rousseaux, S. (2000). Regulated hyperacetylation of core histones during mouse spermatogenesis: involvement of histone deacetylases. Eur. J. Cell Biol. *79*, 950–960.

Hixon, M. L., and Boekelheide, K. (2003). Expression and localization of total Akt1 and phosphorylated Akt1 in the rat seminiferous epithelium. J. Androl. *24*, 891–898.

Hofmann, T. G., Moller, A., Sirma, H., Zentgraf, H., Taya, Y., Droge, W., Will, H., and Schmitz, M. L. (2002). Regulation of p53 activity by its interaction with homeodomain-interacting protein kinase-2. Nat. Cell. Biol. *4*, 1–10.

Ishigaki, S., Fonseca, S. G., Oslowski, C. M., Jurczyk, A., Shearstone, J. R., Zhu, L. J., Permutt, M. A., Greiner, D. L., Bortell, R., and Urano, F. (2010). AATF mediates an antiapoptotic effect of the unfolded protein response through transcriptional regulation of AKT1. Cell Death Differ. *17*, 774–786.

Kang, T. H., Noh, K. H., Kim, J. H., Bae, H. C., Lin, K. Y., Monie, A., Pai, S. I., Hung, C. F., Wu, T. C., and Kim, T. W. (2010). Ectopic expression of X-linked lymphocyte-regulated protein pM1 renders tumor cells resistant to antitumor immunity. Cancer Res. *70*, 3062–3070.

Manning, B. D., and Cantley, L. C. (2007). AKT/PKB signaling: navigating downstream. Cell *129*, 1261–1274.

Meistrich, M. L. (1977). Separation of spermatogenic cells and nuclei from rodent testes. In: Methods in Cell Biology, ed. D.M. Prescott, New York, San Francisco, London: Academic Press, 15–54.

Mueller, J. L., Mahadevaiah, S. K., Park, P. J., Warburton, P. E., Page, D. C., and Turner, J. M. (2008). The mouse X chromosome is enriched for multicopy testis genes showing postmeiotic expression. Nat. Genet. *40*, 794–799.

Niemeyer, P., Tureci, O., Eberle, T., Graf, N., Pfreundschuh, M., and Sahin, U. (2003). Expression of serologically identified tumor antigens in acute leukemias. Leukemia Res. *27*, 655–660.

Obholz, K. L., Akopyan, A., Waymire, K. G., and MacGregor, G. R. (2006). FNDC3A is required for adhesion between spermatids and Sertoli cells. Dev. Biol. *298*, 498–513.

Otipoby, K. L., Sasaki, Y., Schmidt-Supprian, M., Patke, A., Gareus, R., Pasparakis, M., Tarakhovsky, A., and Rajewsky, K. (2008). BAFF activates Akt and Erk through BAFF-R in an IKK1-dependent manner in primary mouse B cells. Proc. Natl. Acad. Sci. USA *105*, 12435–12438.

Partridge, L., and Hurst, L. D. (1998). Sex and conflict. Science *281*, 2003–2008.

Reynard, L. N., Turner, J. M., Cocquet, J., Mahadevaiah, S. K., Toure, A., Hoog, C., and Burgoyne, P. S. (2007). Expression analysis of the mouse multi-copy X-linked gene Xlr-related, meiosis-regulated (Xmr), reveals that Xmr encodes a spermatid-expressed cytoplasmic protein, SLX/XMR. Biol. Reprod. *77*, 329–335.

Russell, L. D., Hikim, A.P.S., Ettlin, R. A., and Clegg, E. D. (1990). Histological and Histopathological Evaluation of the Testis. Cache River Press.

Scavetta, R. J., and Tautz, D. (2010). Copy number changes of CNV regions in intersubspecific crosses of the house mouse. Mol. Biol. Evol. *27*, 1845–1856.

Simpson, A. J., Caballero, O. L., Jungbluth, A., Chen, Y. T., and Old, L. J. (2005). Cancer/testis antigens, gametogenesis and cancer. Nat. Rev. *5*, 615–625.

Singh, B. N., Suresh, A., UmaPrasad, G., Subramanian, S., Sultana, M., Goel, S., Kumar, S., and Singh, L. (2003). A highly conserved human gene encoding a novel member of WD-repeat family of proteins (WDR13). Genomics *81*, 315–328.

Skaletsky, H., Kuroda-Kawaguchi, T., Minx, P. J., Cordum, H. S., Hillier, L., Brown, L. G., Repping, S., Pyntikova, T., Ali, J., Bieri, T., Chinwalla, A., Delehaunty, A., Delehaunty, K., Du, H., Fewell, G., Fulton, L., Fulton, R., Graves, T., Hou, S. F., Latrielle, P., Leonard, S., Mardis, E., Maupin, R., McPherson, J., Miner, T., Nash, W., Nguyen, C., Ozersky, P., Pepin, K., Rock, S., Rohlfing, T., Scott, K., Schultz, B., Strong, C., Tin-Wollam, A., Yang, S. P., Waterston, R. H., Wilson, R. K., Rozen, S., and Page, D. C. (2003). The male-specific region of the human Y chromosome is a mosaic of discrete sequence classes. Nature 423, 825–837.

Sotiropoulou, G., Pampalakis, G., and Diamandis, E. P. (2009). Functional roles of human kallikrein-related peptidases. J. Biol. Chem. 284, 32989–32994.

Spencer, S., Dowbenko, D., Cheng, J., Li, W., Brush, J., Utzig, S., Simanis, V., and Lasky, L. A. (1997). PSTPIP: a tyrosine phosphorylated cleavage furrow-associated protein that is a substrate for a PEST tyrosine phosphatase. J. Cell Biol. 138, 845–860.

Stouffs, K., Tournaye, H., Liebaers, I., and Lissens, W. (2009). Male infertility and the involvement of the X chromosome. Hum. Reprod. Update 15, 623–637.

Suresh, A., Shah, V., Rani, D. S., Singh, B. N., Prasad, G. U., Subramanian, S., Kumar, S., and Singh, L. (2005). A mouse gene encoding a novel member of the WD family of proteins is highly conserved and predominantly expressed in the testis (Wdr13). Mol. Reprod. Dev. 72, 299–310.

Toure, A., Clemente, E. J., Ellis, P., Mahadevaiah, S. K., Ojarikre, O. A., Ball, P. A., Reynard, L., Loveland, K. L., Burgoyne, P. S., and Affara, N. A. (2005). Identification of novel Y chromosome encoded transcripts by testis transcriptome analysis of mice with deletions of the Y chromosome long arm. Genome Biol. 6, R102.

Touré, A., Szot, M., Mahadevaiah, S. K., Rattigan, A., Ojarikre, O. A., and Burgoyne, P. S. (2004). A new deletion of the mouse Y chromosome long arm associated with loss of Ssty expression, abnormal sperm development and sterility. Genetics 166, 901–912.

Yamauchi, Y., Riel, J. M., Stoytcheva, Z., Burgoyne, P. S., and Ward, M. A. (2010). Deficiency in mouse Y chromosome long arm gene complement is associated with sperm DNA damage. Genome Biol. 11, R66.